SUPPORTING INFORMATION

Engineering aluminosilicate's photochromism by quantum chemistry

Pauline Colinet[1], *and Tangui Le Bahers*[1,2]*

[1]Univ Lyon, ENS de Lyon, CNRS, Université Lyon 1, Laboratoire de Chimie, UMR 5182, Lyon, France

[2] Institut Universitaire de France, 5 rue Descartes, 75005 Paris, France

*Corresponding authors: tangui.le_bahers@ens-lyon.fr

Table of Contents

I- Orbitals involved in the photochromism

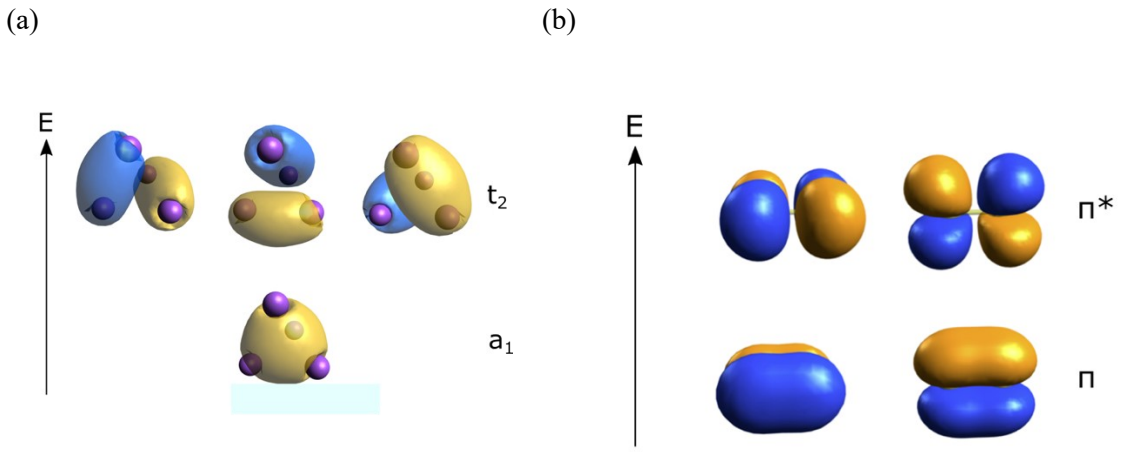

Figure S1: Representation of orbitals isosurfaces (isovalue 0.02 a.u.) (a) trapped electron's orbitals involved in the absorption. (b) π (HOMO) and π^* (LUMO) orbitals of the S_2^{2-} anion. The orbitals are arranged in energy and labelled in symmetry.

II- Spin-orbit coupling calculations.

Using the quasi-degenerate perturbation theory available in ORCA we included spin orbit coupling between the singlet and triplet states obtained using TD-DFT at the CAM-B3LYP/Def2-SVP level of theory.[1] The SOC is calculated in the mean-field formalism. The calculated elements of the coupling matrix (<T|HSO|S>) involving the first triplet state are given in cartesian coordinates for both geometries (white form and colored form), in Tables S1 and S2 respectively.

Table S1: SOC computed between T_1 and other singlet states (in cm^{-1}) for the white geometry.

T	S	Z	X	Y
1	0	(0.00 , -33.60)	(0.00 , -3.48)	(0.00 , -4.85)
1	1	(0.00 , 0.02)	(0.00 , -0.65)	(0.00 , 0.46)
1	2	(0.00 , 16.56)	(0.00 , **-117.22**)	(0.00 , **-114.87**)
1	3	(0.00 , -0.01)	(0.00 , 1.85)	(0.00 , -1.04)

Table S2: SOC computed between T_1 and other singlet states (in cm^{-1}) for the colored geometry.

T	S	Z	X	Y
1	0	(0.00 , -2.30)	(0.00 , 5.38)	(0.00 , 2.32)
1	1	(0.00 , -1.65)	(0.00 , **-117.21**)	(0.00 , **-112.80**)
1	2	(0.00 , 1.57)	(0.00 , 8.68)	(0.00 , 10.10)
1	3	(0.00 , 2.04)	(0.00 , -1.67)	(0.00 , 0.88)

Important values, in bold font, highlight a strong coupling between the first triplet state and the S_1 or S_2 states that correspond to the $^1[S_2^-,V_{Cl}^-]$ electronic state.

III- Cell parameters obtained through geometry optimization of the structures in PBC

Table S3: Cell parameter (Å) from experimental data (exp.) when available[2] and periodic boundary conditions calculation (comp.) using CRYSTAL 17 code and PBE0 functional. X indicates missing experimental values.

Composition	a_{comp} (Å)	a_{exp} (Å)
SiAlCl	8.83	8.89
SiAlBr	8.88	8.96
SiAlI	8.94	9.02
SiGaCl	8.92	8.94
SiGaBr	8.98	9.00
SiGaI	9.04	X
GeAlCl	8.99	9.04
GeAlBr	9.04	9.10
GeAlI	9.10	X
GeGaCl	9.10	X
GeGaBr	9.15	X
GeGaI	9.21	X

IV- Basis sets for the electron in the vacancy at the geometry of both the colorless and colored form

Table S4: Optimized α exponent coefficients of the radial part of 111G(d) basis set in $[Na_4V_X]^{3+}$ for the geometries of colorless and colored forms of different materials.

	White forms				colored forms			
Material	sp #1	sp #2	sp #3	d #4	sp #1	sp #2	sp #3	d #4
SiAlCl	0.065	0.034	0.128	0.050	0.050	0.025	0.232	0.055
SiAlBr	0.031	0.016	0.057	0.044	0.047	0.024	0.367	0.550
SiAlI	0.027	0.014	0.029	0.039	0.043	0.022	0.324	0.053
GeAlCl	0.032	0.016	0.030	0.046	0.051	0.026	0.431	0.055
GeAlBr	0.032	0.016	0.050	0.044	0.047	0.024	0.389	0.054
GeAlI	0.029	0.015	0.030	0.042	0.043	0.022	0.354	0.053
SiGaCl	0.034	0.017	0.063	0.046	0.051	0.026	0.489	0.055
SiGaBr	0.032	0.016	0.037	0.045	0.048	0.024	0.380	0.055
SiGaI	0.030	0.015	0.031	0.043	0.044	0.022	0.331	0.053
GeGaCl	0.033	0.017	0.047	0.046	0.051	0.026	0.483	0.055
GeGaBr	0.032	0.016	0.039	0.045	0.047	0.024	0.429	0.054
GeGaI	0.030	0.015	0.032	0.043	0.044	0.022	0.340	0.053
Na3K	0.069	0.035	0.133	0.069	0.050	0.025	0.212	0.062
Na2K2	0.072	0.036	0.146	0.071	0.050	0.025	0.198	0.065
NaK3	0.076	0.038	0.150	0.075	0.050	0.025	0.175	0.063

V- Benchmark of the range separated hybrid functionals

The choice of CAM-B3LYP to compute the charge transfer transitions energies is based on the following benchmark. The three functionals CAM-B3LYP[3], LC-ωHPBE[4] and ωB97xD[5] characterized by 65%, 100% and 100% of long-range exact exchange respectively were used to computed the activation and bleaching energies of the pristine SiAlCl material and compared to the experimental values. The comparison is presented on Figure S2. CAM-B3LYP appears to be the most appropriate functional to reproduce both energies.

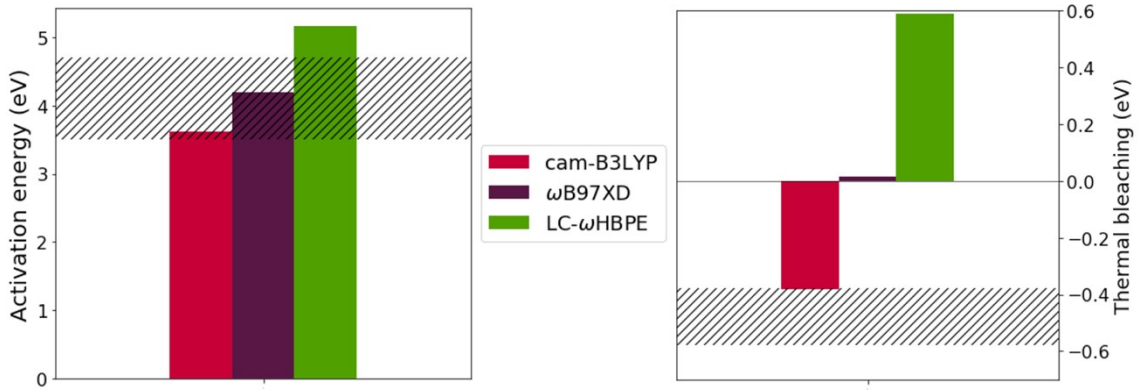

Figure S2: Computed activation (a) and bleaching (b) energies using CAM-B3LYP, LC-ωHPBE and ωB97xD functionals and compared to experimental energies (dashed areas).

VI- Density of states

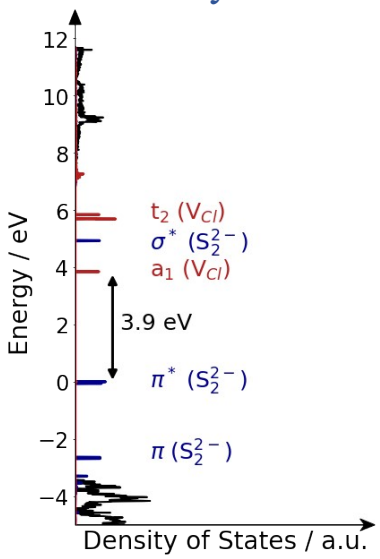

Figure S3: DOS of the supercell containing $S_2^{2-}$and V_{Cl} defects (black) and projected DOS on the S_2^2 (blue) and V_{Cl} (red) orbitals, at the geometry of the colourless form for SiAl composition.

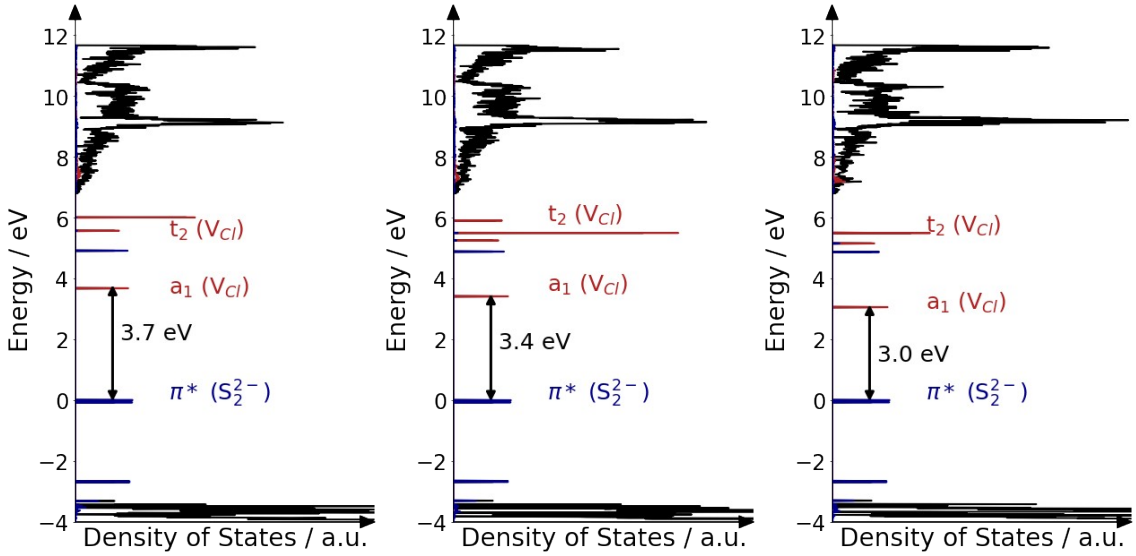

Figure S4: DOS of the supercell containing $S_2^{2-}$and V_{Cl} defects (black) and projected DOS on the S_2^2 (blue) and V_{Cl} (red) orbitals, at the geometry of the colourless form. From left to right : respective DOS for Na_3K, Na_2K_2 and NaK_3 compositions.

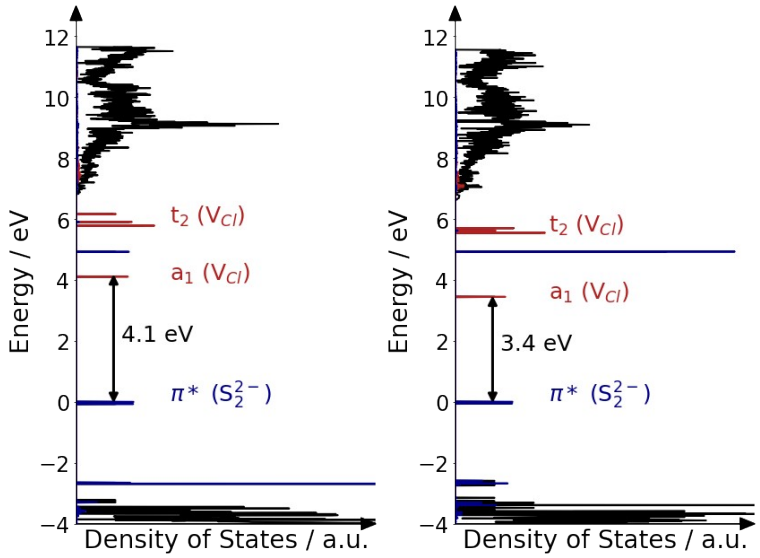

Figure S5: DOS of the supercell containing $S_2^{2-}$and V_{Cl} defects (black) and projected DOS on the S_2^2 (blue) and V_{Cl} (red) orbitals, at the geometry of the colourless form. From left to right : respective DOS for Na_3, and Na_5 compositions.

VII- Computed energies relative to absorption, activation and bleaching processes

Table S5: Computed energies in eV corresponding to the absorption (Eabs), the activation (Ea) and the bleaching for the different materials studied. Eabs are obatined at TD-DFT/B3LYP level of theory, while Ea and Eb are obtained at TD-DFT/CAM-B3LYP level of theory.

Material	Eabs (eV)	Ea (eV)	Eb (eV)
SiAlCl	2.47	3.57	-0.38
SiAlBr	2.36	3.59	-0.38
SiAlI	2.20	3.64	-0.28
GeAlCl	2.24	3.25	-0.41
GeAlBr	2.07	3.32	-0.34
GeAlI	1.91	3.50	-0.28
SiGaCl	2.31	3.30	-0.42
SiGaBr	2.23	3.31	-0.39
SiGaI	2.23	3.52	-0.35
GeGaCl	1.89	3.14	-0.38
GeGaBr	1.79	3.14	-0.34
GeGaI	1.87	3.15	-0.31
K1	2.35	3.58	-0.28
K2	2.62	3.34	-0.20
K3	2.50	3.12	-0.09
Na3	2.30	3.70	-0.29
Na5	3.01	2.73	-0.73

VIII- Comparison between experimental and computed F-center absorption wavelength

Table S6. The computed (TD-DFT/B3LYP) and experimental[2] absorption wavelengths (in nm) along with the signed deviation (in eV).

	$\lambda_{exp.}$(nm)	$\lambda_{comp.}$ (nm)	Difference (eV)
GeAlCl	597.09	554.66	-0.16
GeAlBr	642.04	600.38	-0.13
SiAlBr	556.22	525.11	-0.13
SiAlCl	530.03	502.21	-0.13
SiGaBr	581.11	555.39	-0.10
SiGaCl	556.04	537.55	-0.08

References

1 B. de Souza, G. Farias, F. Neese and R. Izsák, *J. Chem. Theory Comput.*, 2019, **15**, 1896–1904.

2 E. R. Williams, A. Simmonds, J. A. Armstrong and M. T. Weller, *J Mater Chem*, 2010, **20**, 10883–10887.
3 T. Yanai, D. P. Tew and N. C. Handy, *Chem. Phys. Lett.*, 2004, **393**, 51–57.
4 T. M. Henderson, A. F. Izmaylov, G. Scalmani, G. E. Scuseria, *J. Chem. Phys.*, 2009, **131**, 044108.
5 J.-D. Chai and M. Head-Gordon, *Phys. Chem. Chem. Phys.*, 2008, **10**, 6615–6620.